



The human placenta project: Funded studies, imaging technologies, and future directions

Christina L. Herrera^{a,b,*}, Meredith J. Kim^c, Quyen N. Do^d, David M. Owen^{a,b}, Baowei Fei^{d,e,f}, Diane M. Twickler^{a,d}, Catherine Y. Spong^a

^a Department of Obstetrics and Gynecology, UT Southwestern Medical Center, and Parkland Health Dallas, Texas, USA

^b Green Center for Reproductive Biology Sciences, UT Southwestern Medical Center, Dallas, TX, USA

^c University of Texas Southwestern Medical School, Dallas, TX, USA

^d Department of Radiology, UT Southwestern Medical Center, Dallas, TX, USA

^e Advanced Imaging Research Center, UT Southwestern Medical Center, Dallas, TX, USA

^f Department of Bioengineering, University of Texas at Dallas, Dallas, TX, USA

ARTICLE INFO

Part of this work was presented as a poster at the 2022 Annual Meeting of the Society for Maternal-Fetal Medicine.

Keywords:

Human placenta project

Pregnancy

Imaging

Magnetic resonance imaging

Ultrasound

Placental function

Placental structure

ABSTRACT

The placenta plays a critical role in fetal development. It serves as a multi-functional organ that protects and nurtures the fetus during pregnancy. However, despite its importance, the intricacies of placental structure and function in normal and diseased states have remained largely unexplored. Thus, in 2014, the National Institute of Child Health and Human Development launched the Human Placenta Project (HPP). As of May 2023, the HPP has awarded over \$101 million in research funds, resulting in 41 funded studies and 459 publications. We conducted a comprehensive review of these studies and publications to identify areas of funded research, advances in those areas, limitations of current research, and continued areas of need. This paper will specifically review the funded studies by the HPP, followed by an in-depth discussion on advances and gaps within placental-focused imaging. We highlight the progress within magnetic resonance imaging and ultrasound, including development of tools for the assessment of placental function and structure.

1. Introduction

The human placenta functions as a unique multiorgan, simultaneously fulfilling respiratory, renal, hepatic, gastrointestinal, endocrinologic, and immunologic functions. This multifunctional nature modulates both normal pregnancy as well as pathological states that affect both mother and fetus. Consequences of dysfunction include not only immediate sequelae such as insulin resistance, preeclampsia, and growth restriction with concomitant maternal and fetal morbidity, but also longer-term implications for adult neuropsychiatric and cardiovascular health [1–4]. Yet despite its critical role, the human placenta remains one of the least understood organs.

In 2014, the *Eunice Kennedy Shriver* National Institute of Child Health and Human Development (NICHD) recognized this lack of understanding and launched the Human Placenta Project (HPP) [5]. Prior to this

initiative, existing placental research focused on evaluation at delivery; therefore, the principal goal of the HPP was to better understand human placental structure, development, and function in real time across gestation [6]. Other goals identified included development of noninvasive biomarkers for disease prediction, improved understanding of placental implications for long-term health, development of intervention for abnormal placental development, and improved pregnancy outcomes [6]. To achieve such goals, the NIH has held an annual meeting from 2014 to 2018 and then in 2021 to foster multidisciplinary discussion and review progress to date.

Since the founding of the HPP, the NIH has released several funding opportunities via Requests for Applications (RFAs) and Program Announcements (PAR). The purpose of this article is to summarize the studies and resulting publications funded by the HPP as of May 2023. Our goal was to synthesize published data to identify areas of funded

* Corresponding author. Department of Obstetrics and Gynecology, University of Texas Southwestern Medical Center, 5323 Harry Hines Blvd, Dallas, TX, 75390-9032, USA.

E-mail address: christina.herrera@utsouthwestern.edu (C.L. Herrera).

<https://doi.org/10.1016/j.placenta.2023.08.067>

Received 13 March 2023; Received in revised form 16 August 2023; Accepted 19 August 2023

Available online 21 August 2023

0143-4004/© 2023 Elsevier Ltd. All rights reserved.

research, advances in those areas, gaps in current published research, and future directions. Given the extensive nature of the HPP, this article will give a broad overview of HPP-funded research categories and then focus more specifically on studies with application in placental imaging.

2. Materials and methods

A review of all studies and resultant publications funded through the HPP was conducted. Eligible studies were identified via the National Institutes of Health (NIH) Research Portfolio Online Reporting Tools (RePORT) on May 3rd, 2023. Studies were considered eligible if they received funding under a known HPP RFA or PAR. These included the following funded announcements: RFA-HD-15-034, RFA-HD-15-030, RFA-HD-15-031, RFA-HD-16-036, RFA-HD-16-037, RFA-HD-17-004, RFA-HD-17-005, RFA-HD-18-003, RFA-HD-18-004, PAR-18-884, and PAR-18-885. The RFA or PAR was used as the search criteria under Funding Opportunity Announcement (FOA) in RePORT. Search results for both studies and publications were extracted separately into Excel using the RePORT export feature.

Studies were first grouped according to research category. These included imaging, specimen collection, and assays performed (omics). Additional data extracted included: source of data (retrospective or prospective, existing data set), participant (e.g. human, non-human primate, mouse, etc.), cohort (uncomplicated pregnancy, pregnancy exposure), and outcomes (e.g. preeclampsia, fetal growth restriction). Further sub-categorization was then performed (Table 1). For imaging studies, these subcategories included magnetic resonance imaging (MRI), ultrasound (US), and use of other imaging modalities. For each study, it was determined if placental function and/or structure were assessed. Placental MRI function studies were subcategorized into technical development, perfusion, oxygenation, diffusion, and

Table 1
Study categorization strategy.

Category	Subcategory	Purpose	Imaging Subcategory
Imaging	Magnetic Resonance Imaging (MRI)	placental function	technical development perfusion oxygenation metabolism
		placental structure	technical development anatomic assessment
	Ultrasound (US)	placental function	Doppler technical development Power Doppler
		placental structure	qualitative assessment quantitative automated analyses
	Other		
Specimen	Blood/extracellular vesicles		
	Peripheral cells		
	Tissue		
	Urine		
	Amniotic fluid		
Omics	Epigenome (e.g DNA, cfDNA)		
	Transcriptome (e.g RNA)		
	Proteome (e.g Mass spectrometry, Antibody-based)		
	Metabolome (e.g Mass spectrometry)		
	Lipidome (e.g Mass spectrometry, profiling)		
	Microbiome		

metabolism. Placental MRI structure studies were divided among technical development and anatomic assessment. Placental US function studies received the following subcategories: Doppler, technical development, and Power Doppler. Lastly, placental US structure studies were organized as follows: qualitative assessment and quantitative automated analyses.

Publications were categorized similarly after determining if the study focus was placental or non-placental. Placental focus was defined as imaging of the placenta *in vivo* or *ex vivo* for functional or structural information, use of placental tissue for analysis, and/or correlation of expression with placental tissue. Article type as well as two additional categories were collected. Article type was defined as original research, expert review, systematic review, and case report. The two additional categories were technical development and other to accommodate associated literature of funded studies that were not placental-specific in nature. Technical development encompassed work in other analytic procedures that could be used for placental analysis, particularly on the microscopic to nanoscopic level. Imaging publications that were not placental-focused were excluded from this review. Each original research publication was reviewed by at least two of the authors (C.L.H. and M.J.K.) and assessed for purpose, principle finding, major advance, and identified areas of need. Expert consultation and summative review were then performed (D.M.T., B.F., C.Y.S.).

3. Results

A total of 41 studies were funded by the Human Placenta Project with \$101.7 million dollars awarded. There were 459 resultant publications as of May 3rd, 2023 (Table 2). Studies were: imaging only (12, 29%) totaling \$32.5 million in funding; imaging and specimen collection with or without planned assay application (11, 27%) with \$32 million in funding; or specimen collection with planned assay application (18, 44%) with \$37.2 million in funding (Fig. 1). Publications typically focused on either imaging (164, 36%) or specimen collection with assay application (177, 39%) as opposed to combined data together (29, 6%). Slightly less than half of the publications (205, 45%) were specifically focused on the placenta. Those not directly related to the placenta were primarily focused on imaging and analytic techniques to enhance understanding of the placenta or validate techniques that could be applied to the placenta. Examples include MR technical development for metabolism, perfusion, oxygenation, diffusion and segmentation in phantoms and nonpregnant adults and work on acoustofluidics, exosome isolation, DNA or miRNA extraction.

Table 2
HPP studies, funding, and resultant publications by research category.

Research Category	Number of Studies Funded	Amount Allocated (millions)	Number of Resultant Publications	Placental Publications
Imaging	12 (29%)	\$32.5 (32%)	165 (37%)	75 (37%)
Imaging + Specimen	6 (15%)	\$18.8 (18%)	23 (5%)	15 (7%)
Imaging + Specimen + Omics	5 (12%)	\$13.2 (13%)	8 (2%)	8 (4%)
Specimen + Omics	18 (44%)	\$37.2 (37%)	179 (39%)	86 (42%)
Technical Development ^a			43 (9%)	1 (0%)
Other			41 (9%)	20 (10%)
Total	41	\$101.7	459	205

^a Technical Development encompasses work in acoustofluidics, 3D simulation, and other non-omic analytic procedures that could be used for placental analysis, particularly on the microscopic to nanoscopic level.

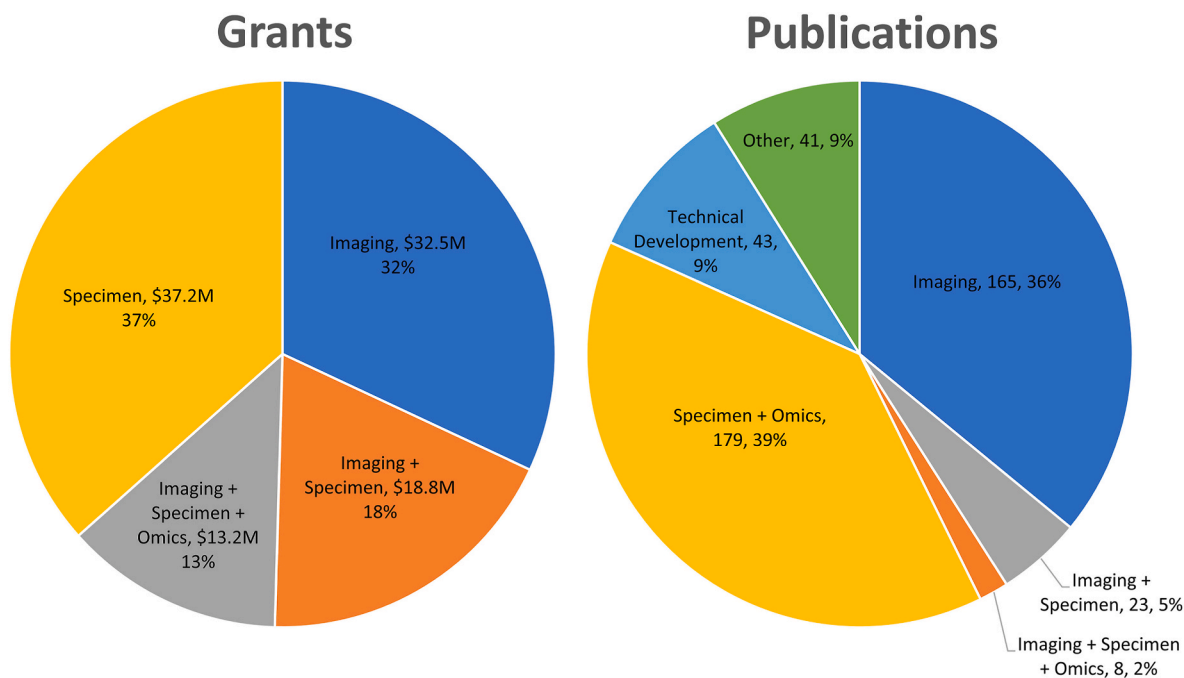


Fig. 1. Pie chart representations of funding and resultant publications by research category.

4. Imaging

There were 23 studies and 196 publications that utilized imaging, comprising 56% and 43% of all HPP studies and publications, respectively. Studies were MR only (12, 52%) with \$32.4 million in funding; MRI combined with another modality (4, 17%) with \$15.8 million in funding; and ultrasound only (7, 30%) with \$16.3 million in funding. Publications mirrored this funding application (Table 3). Ninety-eight of the 196 imaging publications (50%) were placental-focused with the majority either MR (53, 54%) or ultrasound alone (25, 26%). Eighty-eight of these publications were original research articles [7–94]; 3 were systematic reviews on ultrasound [95–97]; 4 were expert reviews on MR oxygenation, MR quantitative susceptibility mapping, US-guided photoacoustic imaging of the placenta, and multimodal placental imaging respectively [98–101]; 2 were corrections to previously published articles [102,103]; and 1 was a case report [104].

Table 3

HPP studies, funding, and resultant publications in imaging. Examples of other imaging include cystoscopy, positron emission tomography, color power angiography, contrast-enhanced and micro computed topography. MRI = magnetic resonance imaging, US = ultrasound.

Imaging	Number of Studies Funded	Amount Allocated (Millions)	Number of Resultant Publications	Placental Publications	Placental Original Research
MRI	12 (52%)	\$ 32.4 (50%)	119 (61%)	53 (54%)	49
MRI + US	2 (9%)	\$ 8.3 (13%)	9 (5%)	7 (7%)	6
MRI + US + other	1 (4%)	\$ 4.3 (7%)	2 (1%)	1 (1%)	0
MRI + other	1 (4%)	\$ 3.2 (5%)	7 (4%)	3 (3%)	3
US	7 (30%)	\$ 16.3 (25%)	43 (22%)	25 (26%)	22
US + other			4 (2%)	3 (3%)	3
Other			12 (6%)	6 (6%)	5
Total	23	\$64.5	196	98	88

5. Magnetic resonance imaging

There were 58 original research articles that utilized MRI [7–64], all but six [59–64] of which characterized aspects of placental function and 34 aspects of placental structure [7–18,29–39,47–51,59–64] (Table 4). Within placental function, 19 studies covered aspects of technical development [7–25], 15 placental perfusion [26–40], 19 placental oxygenation [12,36–53], 5 placental diffusion [34,41,47,51,54], and 4 placental metabolism [55–58]. Within placental structure, 8 studies focused on aspects of technical development [13–18,59–61] and 28 anatomic assessment [7–13,29–39,47–51,62–64].

Table 4

Original research publications in imaging by subcategory. 14 studies included more than one modality: 7 magnetic resonance imaging (MRI) and ultrasound (US), 3 US and other, and 4 MRI and other.

Category	Modality	Purpose	Subcategory
Imaging (88)	Magnetic Resonance Imaging (58)	placental function (52)	technical development (19)
			perfusion (15)
		placental structure (34)	oxygenation (19)
Ultrasound (32)	placental function (24)	diffusion (5)	
		metabolism (4)	
		technical development (9)	
Other (12)	placental structure (13)	anatomic assessment (26)	
		Doppler (17)	
		technical development (2)	
Other (12)	placental structure (13)	power Doppler (6)	
		qualitative assessment (5)	
		quantitative automated analyses (9)	

6. MR advances

6.1. Placental function

6.1.1. Technical development

MR technical development from the HPP has worked with animals, retrospective data sets, and prospective recruitment of pregnant people to assist in the development of novel techniques for assessment of placental function. In animals, work has been done in pregnant mice to characterize angiogenesis at implantation [7], biotin transporter activity [8], and placental blood volumes [23]. Feasibility and proof-of-principle studies of ferumoxytol-enhanced MRI at the maternal-fetal interface were found to have minimal effects on placenta or fetus [9], correlate oxygenation with spiral arteries [10], and evaluate placental inflammation in pregnant rhesus macques [11,25].

Human characterization worked toward assessment with uterine activity during pregnancy [14], motion correction [15–17,24], placental flattening [18], and automated segmentation of the placenta to obtain functional imaging data [19]. Other studies investigated prospective *in vivo* assessment of placental dysfunction via hemoglobin dissociation curves [20] and blood hemodynamics [12]. Assessment of *in-vivo* fetal-blood oximetry was accomplished by utilizing a calibration equation obtained from T_2 and HbO₂ values of ex-vivo fetal blood from umbilical cord blood samples [21]. Further human feasibility data has included assessment of diffusion using intravoxel incoherent motion (IVIM) [12,13] and ex-vivo assessment of perfusion of the umbilical artery and intervillous space [22].

6.1.2. Perfusion

Multiple HPP investigators have worked to develop *in vivo* animal and human models for assessment of placental perfusion. In animals, these include application of dynamic contrast-enhanced (DCE-MRI) with gadoteridol [28,29,37–40] and ferumoxytol [31,35], arterial spin labeling (ASL) via flow-sensitive alternating inversion recovery (FAIR) [31], and 4D flow MRI [32] for assessment of perfusion in pregnant macaques. DCE-MRI was found to demonstrate significantly reduced perfusion in pregnant macaques with fetal growth restriction (FGR) [38], chronic first trimester alcohol exposure [37,40], and with pathology due to Zika virus [35,39]. In addition, DCE-MRI demonstrated significantly reduced perfusion in pregnant macaques on a chronic western-style diet, but this reduction could be ameliorated with diet reversal [28]. DCE-MRI also demonstrated reduced perfusion with aberrant uterine contractility in pregnant rats [36] and mouse models of preeclampsia and growth-restriction [34]. Based on current modeling [28,29,37–39] and the large molecular size of ferumoxytol [31,35], DCE-MRI primarily reflects the maternal side of placental blood flow.

Various methods have been explored for the assessment of perfusion measurement in uncomplicated human pregnancy. These include a free-breathing pseudocontinuous (pCASL) ASL technique [26] and a velocity-selective method (VS-ASL) [27]. In the setting of ischemic placental disease (gestational hypertension, preeclampsia, and FGR), pCASL-based perfusion was found to significantly decrease when measured at 16 weeks [30,33]. pCASL reflects maternal-side placental blood flow, while VS-ASL reflects both maternal and fetal blood flow.

6.1.3. Oxygenation

Similar to perfusion, animal and human models of placental oxygenation have also been developed by HPP investigators. Overlap can be seen among groups assessing perfusion and oxygenation metrics [36–39,47]. Oxygenation has been assessed using blood oxygen level-dependent (BOLD) imaging via relaxometry with T_2^* and R_2^* ($1/T_2^*$) mapping [36–39,41,43,46–52]. Others used BOLD to assess oxygen kinetics and have assessed time to plateau (TTP) [42,44]. Oxygenation has also been measured through quantitative susceptibility mapping (QSM) [12,45]. Combined T_1 and T_2 -mapping has also been explored for representation of oxygenation, as T_2 is not impacted by

local magnetic field inhomogeneities like T_2^* [53].

Similar to effects on perfusion, reduced oxygenation was also observed in pregnant macaques with FGR [38] and chronic first trimester alcohol exposure [37,40] as well as with aberrant uterine contractility in pregnant rats [36]. In Zika-infected pregnant macaques, higher-than-expected oxygenation of maternal blood was found within the placenta, which the authors suggested may reflect decreased oxygen permeability or decreased fetal demand in affected placentas [39].

In humans, global placental T_2^* has been shown to decrease over gestation. Recently T_2^* has been further described as decreasing continuously from a high plateau level early in gestation, through an inflection point at 30 weeks, and approaching a second, lower plateau in late gestation, based off a cohort of 316 pregnancies [50]. In a study that included anterior and fundal placentas, there was a decline in T_2^* from center to periphery in each individual placental lobule, thought to represent oxygen exchange between maternal and fetal circulation within the intervillous space [47]. Regarding clinical correlation, T_2^* is significantly reduced in placentas with adverse outcomes [48,50], maternal chronic hypertension [41], and congenital heart disease [52] compared to unaffected placentas. Variation in R_2^* has been suggested based on placental location, with lower values in anterior compared to posterior placentas derived from 3D volumetric analysis [43]. Maternal position and contractions have also been found to cause variation, with global and regional differences in T_2^*/R_2^* and regional time to plateau (TTP) [44,46,49]. Moreover, decreases in placental T_2^* with contractions have been found to correlate with decreased T_2^* in the fetal liver and brain [46]. In addition, with maternal hypoxemia, longer TTP has been observed in the smaller of discordant monozygotic twin pairs [42].

6.1.4. Diffusion

Diffusion-weighted (DW) MRI has been investigated for its complementary information, often used as part of a combined approach for functional data. Diffusion-weighted imaging (DWI) is sensitive to water motion which may include intra- and extra-cellular water diffusion and may be a marker for early perfusion while also reflecting *in vivo* morphology. In mouse models of preeclampsia and growth-restriction, similar to perfusion, diffusion was also decreased in these diseased states [34]. In human pregnancy, examples included combined relaxometry-diffusion using T_2^* and apparent diffusion coefficient (ADC) mapping [47,51] and T_1 and ADC mapping, with an acquisition time under 2 min [54]. These studies describe trends for decreases in T_2^* and diffusivity with increasing gestational age [47] and placental disease (preeclampsia, fetal growth restriction) [51,54]. Another combined MR examination (T_2 -weighted imaging, T_2^* , T_1 and ADC mapping) recently demonstrated varying placental phenotypes in pregnant individuals with chronic hypertension; however, values overlapped with the control group of healthy pregnant individuals [41].

6.1.5. Metabolism

Work on placental metabolism within MR imaging is in its early stages. Preliminary work has been applied to look at hyperpolarized ¹³C MRI in animals for the metabolism of substrates such as pyruvate, lactate, and urea in the placenta [55–57]. Luo et al. demonstrated feasibility of glucose chemical saturation exchange transfer (CEST) in humans for non-invasive measurement of glucose transport in the placenta [58].

6.2. Placental structure

6.2.1. Technical development

Efforts to better delineate placental structure included some animal and many human pregnancies. Liposomal gadolinium was used in a pregnant mouse model to specify the retroplacental clear space as well as morphologic volume changes thorough gestation [59,61]. Algorithms for placental flattening [18,60] and motion correction [15,17] were used for structural assessment as well, with development of placental

volume reconstruction using a dataset of human fetuses with minor and severe motion [16] and characterization of uterine activity during pregnancy [14]. Anisotropic IVIM models were applied for assessment of human placental microvascular structure and tissue microstructure [13].

6.2.2. Anatomic assessment

Most studies relied on manual regions of interest (ROIs) for placental identification. Similarly, division of the placenta into anatomic units has occurred through manual and post-processing techniques. Manual ROIs with DCE-MRI have been applied for placental lobe and cotyledon specification [10–12,29,34,35,37–39], volume measurements [29,35], maternal and fetal tissue delineation [9], implantation site identification [7], and for delineation of uterine vasculature as well as the intervillous space [31,32]. Others have proposed dividing the placenta into various compartments via mathematical modeling [8]. In human placentas, manual segmentation has been used for volume quantification [30,33,35,47–50] and anatomic division [12,13,36,47,51,64]. Recently, automated placental segmentation has begun and has been applied to placental volumes [62].

7. MR gaps

When considering the gaps remaining after advances from the HPP, it is useful to frame current knowledge in the context of Standards for the Reporting of Diagnostic Accuracy Studies (STARD) [105]. Diagnostic testing is most useful when a medical test is available that provides useful information on the health of the patient, a target condition is defined, there is an accepted clinical reference standard, the test has sufficient sensitivity and specificity, and testing results in a clear intention for use (diagnosis, screening, prediction, prognosis).

On this basis there are several current limitations in MR knowledge. Medical testing is available, but there is not yet an agreed upon best approach and much is needed in the manner of technical development prior to pursuit of diagnostic testing. For MR-based techniques challenges include the need for correction or adjustment due to maternal breathing, fetal motion, contractions, maternal position, placental position. Variation in maternal blood volume, blood flow, blood oxygenation, and blood glucose levels pose difficulty with functional data assessment. The optimal MR approaches for perfusion, oxygenation, and diffusion are not yet clear. There is also variation among 2D versus 3D measurement ascertainment and in determination of ROIs [19,53]. In addition, most ROIs previously were manually segmented. Movement towards automatic segmentation can remove inherent subjectivity in measurement [19,62]. Finally, current published studies primarily assessed global measurements, though evidence suggests that there is likely regional anatomic variation in placental function [22,33,46]. Whether the measurement needs to be cotyledon-specific, maternal-sided, fetal-sided, based out of the intervillous space, or a composite of these areas also remains to be determined. Due to these issues, further optimization and standardization of MR technique is needed to enable comparison of the literature and prior to clinical application for diagnostic testing.

There is also a need to establish a clinical reference standard for MR functional imaging, specifically gestational-age adjusted normal ranges [40,41,48]. Some headway has been made for T_2^* [50]. Larger sample size of uncomplicated human pregnancies are still needed, as small sample size is a limitation of much of the current published data [12,17,21,26,27,43,45,49,51,52]. In addition, larger cohorts of disease states are also required, as the composites of adverse outcomes are not sufficiently predictive at present [50]. As these sample sizes grow, further work will elucidate if sufficient sensitivity and specificity can be found to aid prediction of and ultimately intervention for placental-mediated disease.

8. Ultrasound

There were 32 original research publications that utilized ultrasound [28–30,37–40,65–89]: 24 covered aspects of placental function [28–30,37–40,65–81] and 13 placental structure [28,39,79–89]. Within placental function, 17 focused on Doppler [28–30,37–40,65–74], 3 on technical development [28,75], and 6 on Power Doppler [76–81]. For placental structure, 4 has components of general assessment [28,39,79,80,82] and 9 ultrasound studies worked on automation [80,81,83–89].

9. US advances

9.1. Placental function

9.1.1. Doppler

Doppler has been used by many for attempted quantification of uteroplacental blood flow with limited association to clinical outcomes. Most commonly, Doppler has been used to assess uterine artery pulsatility index as a marker for impedance of uteroplacental circulation with mixed success [28,30]. Uterine artery pulsatility index does vary by fetal sex [71]. Another common method described has included calculated blood flow of both the uterine artery (maternal vessel, termed cQ_{UA}) and umbilical vein (fetal vessel, termed cQ_{UV}) [28,29,37,38,40]; however, measurements limited to these two major vessels seemingly lack sensitivity to detect placental dysfunction, likely as they are not completely reflective of the intervillous space [39,66].

Others have studied umbilical artery (UA) velocity wave reflections as a potential marker of dysfunction, hypothesizing that elevated placental vascular resistance may be observed as an elevated pulse wave from the fetal heart [65,70]. Initial work was undertaken in mouse models [65,67] and found wave reflections more sensitive to changes in placental vascular resistance than UA pulsatility index [68] and correlated negative flow reflected waveforms with increased terminal impedance in the placenta [74]. Subsequent studies transitioned to human pregnancy [69,70], and have found significantly elevated wave reflections in pathologic outcomes of maternal vascular malperfusion and fetal vascular malperfusion [72].

Superb microvascular imaging (SMI) has been paired with color Doppler to determine resistive indices of the spiral arteries and intervillous space, which were significantly more elevated in the late third trimester for preeclampsia and fetal growth restriction [73]. However, the value added of this finding is limited, given the association is only with late gestational age and it has not yet been validated by larger studies.

9.1.2. Technical development

Work toward functional assessment in ultrasound included modeling of flow from the spiral arteries into the intervillous space throughout gestation based on pulsed wave Doppler ultrasound in uncomplicated pregnancies at 11–13 weeks [75]. The model found that villous structure appears under the influence of spiral artery blood flow, as free spaces must develop distal to spiral arteries to allow blood flow to penetrate among villous tree branching.

Contrast-enhanced ultrasound with microbubbles has been used in pregnant macaques to visualize individual spiral arteries and determine spiral artery transit time [28]. Transit time was found to be increased in those exposed to a chronic Western-style diet, correlating with decreased placental perfusion observed on MR imaging and decreased uterine artery blood flow as determined by Doppler [28].

9.1.3. Power Doppler

Power Doppler (PD) can be used as a measure of vascularity in tissue. 3-dimensional PD (3D PD) has been applied in the first trimester (11–13 weeks) in human pregnancy for assessment of placental vascularity. Published assessments include a diagnostic marker for placenta accreta spectrum along the uteroplacental interface, termed the largest area of

confluent 3D PD signal (A_{con}). In PAS, A_{con} is quantitatively increased, in keeping with known neovascularization along the bladder-serosal interface [76]. This measurement was found to be best achieved with a filled bladder as opposed to unfilled [77]. Another PD-derived metric is 3D fractional moving blood volume (3D-FMBV), a validated method for estimating tissue perfusion using ultrasound [80]. Applied at the uteroplacental interface, pregnancies that develop preeclampsia have reduced 3D-FMBV whereas pregnancies with small for gestational age (SGA) pregnancies resulted in similar vascularity to normotensive appropriate for gestational age (AGA) pregnancies [80]. This technique was recently automated [81]. Also using automated 3D PD, spiral artery jet number, area, and PD area close to the uteroplacental interface (2–3 mm) was found to be smaller in preeclampsia and some pregnant individuals with SGA pregnancies as compared to those with normotensive AGA pregnancies [79].

In contrast to 3D approaches, others have used a 2D approach and demonstrated that placental vascular pulsatility varies throughout the maternal cardiac cycle [78]. As pulsatility can reflect vascular modeling and resistance, this method holds promise as a potential marker for abnormal spiral artery remodeling that enables inter-subject comparison, as patients can serve as their own controls. Such insight is important as this cycle variation is not yet well accounted for in 3D techniques.

9.2. Placental structure

9.2.1. Qualitative assessment

Some features of placental structure were also assessed in US studies. In animals, contrast-enhanced ultrasound has been used for spiral artery identification [28,39]. Similar to vascularity, 3D-derived placental volume has been used in the assessment of the first trimester placenta in human pregnancy. Placentas of those who go on to develop preeclampsia and small for gestational age pregnancies had smaller placentas than normotensive AGA pregnancies [80]. Number of spiral arteries and size (cross-sectional area) have also been determined using 3D PD ultrasound data [79]. Ultrasound has also been used to aid in the application of optical spectroscopy (see Other Imaging) for delineation of placental oxygenation to provide tissue layer morphology (e.g. adipose, rectus/uterus, and placental tissue) and physiologic properties [82].

9.2.2. Quantitative automated analyses

A move toward automated tools for standardized structural evaluation was observed in many of the ultrasound studies. Described in the literature are algorithms for semi-automated 3D placental volume assessment [80,88], structural detection of the placenta, myometrium, and subcutaneous tissue [83], automated lacunae localization in PAS [84], knowledge-guided pretext learning for the uteroplacental interface in PAS [85], and now fully automated placental volumes using deep learning [81,86,87,89]. The value added in prediction for small for gestational age by first trimester volume is potentially promising. While the area under the curve for first trimester volumes has ranged from 0.61 to 0.78,^{86,89} this improved significantly to 0.897 when added to additional clinical modeling [89].

10. US gaps

Similar limitations as outlined for MR exist within US data. The ideal US test for placental disease is unknown and there remain several technical limitations. There is a need to standardize US machine settings, determine the best method for measurement and of which space (maternal, fetal, and intervillous), and automate measurement ascertainment. Reduction of operator dependency will be necessary prior to larger clinical trials given limited reproducibility or replication. Additional consideration for 3D PD includes the pulsatile nature of the vascular bed [78]. Techniques must also be developed that account for variation in placental location [78] and impact of fetal sex given

recently discovered differences [71].

For development of diagnostic testing, larger sample sizes will be needed to create a reference standard that is distinguishable from disease states, as most studies are limited to small sample sizes [72,73,81,83,86] and/or in uncomplicated human pregnancy [67,68,81]. Larger and newer data sets are need for automation [87,89] given the rapid evolution of technology and for disease association.

11. Other imaging

There were 12 studies that utilized other imaging techniques aside from MR and US for evaluation of the placenta [8,23,61,63,67,74,82,90–94]. X-ray micro-computed tomography (CT) [67,74,90–92] has been used for elucidation of placenta vasculature in animal models. A combination of micro-CT and scanning electron microscopy has been used to assess placental adaptations to chronic fetal hypoxia in mice [91]. Pre-operative cystoscopy for the assessment of PAS severity when placentation is over the prior scar and in proximity to the bladder wall has also been investigated [93].

Often additional imaging techniques were used to complement or validate MR findings. For example, in pregnant mice, contrast-enhanced CT has been used to validate placental fractional blood volume [23], retroplacental clear space [61], and placental margins [63] as determined by contrast-enhanced MR with liposomal gadolinium, and positron emission topography was used to correlate with biotin transporter activity [8]. Use of such imaging in human pregnancy remains limited to due ionizing radiation exposure.

An evolving field for placenta evaluation is optical imaging, with many preclinical investigations reported. More recent clinical applications have included optic spectroscopy [82] coupled with ultrasound imaging and photoacoustic imaging [94] for monitoring of placental oxygenation.

12. Limitations

We herein report on all placental-focused imaging publications resulting from HPP funding, though we recognize that this does not encompass all placenta research and advancement. Pre-clinical studies not directly applied to the placenta are not included. All publications were reviewed based on the NIH Reporter system. It is possible that manuscripts not yet associated within this system but published are not included in this review.

13. Future directions

The HPP has enhanced our real-time knowledge of the placenta, but numerous gaps remain. Next steps include determining the most effective non-invasive methods for assessment of placental function. The technical changes faced by current imaging methods must be addressed, including determining the appropriate regions of interest for measurement. Translation of MR and US to clinical application for diagnostic testing at present is likely hindered by the inter-observer variability and different institutional protocols. Therefore, working toward reproducible standardized ascertainment, automated analyses, and reporting is paramount. This includes creating an environment that fosters encouragement of shared algorithms, machine software, calculations, and methods. More systemic issues must also be acknowledged that limit current innovation – profit-driven obstacles at the manufacturer level including machine-specific software and current and historical underfunding for women's health research [106].

As processes become better defined, an additional step will be to reliably and reproducibly correlate imaging metrics with normal placental function throughout gestation and with placental disease pathology. Only then can clear associations with disease be solidified and the ultimate goal of understanding the placental disease achieved – a clinically useful tool for disease prediction that enables intervention for

such pathology.

Funding

This research did not receive any specific grant from funding agencies in the public, commercial, or not-for-profit sectors. CLH is supported by K23HD103876 and L30HD109864 and QND by K25HD104004 for placental research.

Declaration of competing interest

The authors declare that they have no known competing financial interests or personal relationships that could have appeared to influence the work reported in this paper.

Abbreviation guide

HPP	Human Placenta Project
NICHD	National Institute of Child Health and Human Development
FGR	Fetal growth restriction
MRI	Magnetic resonance imaging
US	Ultrasound
DCE-MRI	Dynamic contrast enhanced MRI – MR acquisition obtained during the passage of a contrast agent
ASL	Arterial spin labeling: noninvasive perfusion technique in which endogenous water is labeled upon a selected plane via radiofrequency and magnetic field gradient pulses
pCASL	Pseudocontinuous ASL: ASL method with enhanced signal and reduced signal-to-noise ratio compared to pulsed labeling
VSASL	Velocity-selective ASL: noninvasive perfusion technique in which blood is labeled based on velocity
FAIR	Flow-sensitive alternating inversion recovery: noninvasive ASL perfusion technique in which pulse sequences generate tagged and control images
BOLD-MRI	Blood oxygen level-dependent MRI: noninvasive technique that when applied in the placenta reflects oxygenation based on changes in the ratio of oxyhemoglobin to deoxyhemoglobin
QSM	Quantitative Susceptibility Mapping: MRI measurements of the magnetic susceptibility of a tissue. For oxygenation, it is directly related to the hemoglobin saturation
ROI	Region of interest
T₂*	Time constant for the decay of transverse magnetization caused by a combination of spin-spin relaxation and magnetic field inhomogeneity. For oxygenation, based on changes between paramagnetic deoxyhemoglobin and non-paramagnetic oxyhemoglobin
R₂*	Apparent proton relaxation rate, equivalent to 1/T ₂ *
TTP	Time to Plateau: time that the signal change due to regional oxygenation reaches to the plateau
DWI	Diffusion-weighted imaging: MRI acquisition based on measuring the random Brownian motion of water protons within a voxel of tissue
IVIM	Intravoxel incoherent motion: characterizing the microscopic motions of water in each image voxel, using diffusion-weighted imaging
ADC	Apparent diffusion coefficient: measure of the magnitude of diffusion of water protons within tissue, calculated using diffusion-weighted imaging
CEST	Chemical exchange saturation transfer: MRI contrast approach in which endogenous or exogenous compounds with exchangeable protons are selectively saturated and, after transfer of this saturation, detected through an attenuated water signal
3D-FMBV	3-dimensional fractional moving blood volume

References

- [1] S. Rees, T. Inder, Fetal and neonatal origins of altered brain development, *Early Hum. Dev.* 81 (9) (2005) 753–761.
- [2] D.J. Barker, K.L. Thornburg, Placental programming of chronic diseases, cancer and lifespan: a review, *Placenta* 34 (10) (2013) 841–845.
- [3] L.M. Amaral, M.W. Cunningham Jr., D.C. Cornelius, B. LaMarca, Preeclampsia: long-term consequences for vascular health, *Vasc. Health Risk Manag.* 11 (2015) 403–415.
- [4] P. Kratimenos, A.A. Penn, Placental programming of neuropsychiatric disease, *Pediatr. Res.* 86 (2) (2019) 157–164.
- [5] A.E. Guttmacher, Y.T. Maddox, C.Y. Spong, The Human Placenta Project: placental structure, development, and function in real time, *Placenta* 35 (5) (2014) 303–304.
- [6] A.E. Guttmacher, C.Y. Spong, The human placenta project: it's time for real time, *Am. J. Obstet. Gynecol.* 213 (4 Suppl) (2015) S3–S5.
- [7] G. Cohen, R. Hadas, R. Stefania, A. Pagoto, S. Ben-Dor, F. Kohen, D. Longo, M. Elbaz, N. Dekel, E. Gershon, S. Aime, M. Neeman, Magnetic resonance imaging reveals distinct roles for tissue transglutaminase and factor XIII in maternal angiogenesis during early mouse pregnancy, *Arterioscler. Thromb. Vasc. Biol.* 39 (8) (2019) 1602–1613.
- [8] B.E. Noam, L. Marina, B.E. Inbal, G. Ofra, B.L. Jennifer, F.R. Solana, A. Tolulope, C.A. Nicholas, B. Rebecca, L.E. Suzanne, G.R. Joel, N. Michal, Novel multimodal molecular imaging of Vitamin H (Biotin) transporter activity in the murine placenta, *Sci. Rep.* 10 (1) (2020), 20767.
- [9] S.M. Nguyen, G.J. Wiepaz, M. Schotzko, H.A. Simmons, A. Mejia, K.D. Ludwig, A. Zhu, K. Brunner, D. Hernando, S.B. Reeder, O. Wieben, K. Johnson, D. Shah, T. G. Golos, Impact of ferumoxytol magnetic resonance imaging on the rhesus macaque maternal-fetal interface, *Biol. Reprod.* 102 (2) (2020) 434–444.
- [10] M.C. Schabel, V.H.J. Roberts, J.O. Lo, S. Platt, K.A. Grant, A.E. Frias, C. D. Kroenke, Functional imaging of the nonhuman primate placenta with endogenous blood oxygen level-dependent contrast, *Magn. Reson. Med.* 76 (5) (2016) 1551–1562.
- [11] A. Zhu, S.B. Reeder, K.M. Johnson, S.M. Nguyen, S.B. Fain, I.M. Bird, T.G. Golos, O. Wieben, D.M. Shah, D. Hernando, Quantitative ferumoxytol-enhanced MRI in pregnancy: a feasibility study in the nonhuman primate, *Magn. Reson. Imaging* 65 (2020) 100–108.
- [12] N.S. Dellschaft, G. Hutchinson, S. Shah, N.W. Jones, C. Bradley, L. Leach, C. Platt, R. Bowtell, P.A. Gowland, The haemodynamics of the human placenta in utero, *PLoS Biol.* 18 (5) (2020), e3000676.
- [13] P.J. Slatore, J. Hutter, L. McCabe, A.D.S. Gomes, A.N. Price, E. Panagiotaki, M. A. Rutherford, J.V. Hajnal, D.C. Alexander, Placenta microstructure and microcirculation imaging with diffusion MRI, *Magn. Reson. Med.* 80 (2) (2018) 756–766.
- [14] T. Martin, C. Janzen, X. Li, I. Del Rosario, T. Chanlaw, S. Choi, T. Armstrong, R. Masamed, H.H. Wu, S.U. Devaskar, K. Sung, Characterization of uterine motion in early gestation using MRI-based motion tracking, *Diagnostics* 10 (10) (2020).
- [15] J. Hutter, D.J. Christiaens, T. Schneider, L. Cordero-Grande, P.J. Slatore, M. Deprez, A.N. Price, J.D. Tournier, M. Rutherford, J.V. Hajnal, Slice-level diffusion encoding for motion and distortion correction, *Med. Image Anal.* 48 (2018) 214–229.
- [16] A. Uus, T. Zhang, L.H. Jackson, T.A. Roberts, M.A. Rutherford, J.V. Hajnal, M. Deprez, Deformable slice-to-volume registration for motion correction of fetal body and placenta MRI, *IEEE Trans. Med. Imag.* 39 (9) (2020) 2750–2759.
- [17] R. Liao, E.A. Turk, M. Zhang, J. Luo, P.E. Grant, E. Adalsteinsson, P. Golland, Temporal registration in in-utero volumetric MRI time series, *Med Image Comput Assist Interv* 9902 (2016) 54–62.
- [18] S.M. Abulnaga, E.A. Turk, M. Bessmeltsev, P.E. Grant, J. Solomon, P. Golland, Placental flattening via volumetric parameterization, *Med Image Comput Assist Interv* 1767 (2019) 39–47.
- [19] M. Pietsch, A. Ho, A. Bardanzellu, A.M.A. Zeidan, L.C. Chappell, J.V. Hajnal, M. Rutherford, J. Hutter, APPLAUSE: automatic prediction of PLAcental health via U-net segmentation and statistical evaluation, *Med. Image Anal.* 72 (2021), 102145.
- [20] R. Avni, O. Golani, A. Akselrod-Ballin, Y. Cohen, I. Biton, J.R. Garbow, M. Neeman, MR imaging-derived oxygen-hemoglobin dissociation curves and fetal-placental oxygen-hemoglobin affinities, *Radiology* 280 (1) (2016) 68–77.
- [21] A.E. Rodríguez-Soto, M.C. Langham, O. Abdulmalik, E.K. Englund, N. Schwartz, F.W. Wehrli, MRI quantification of human fetal O(2) delivery rate in the second and third trimesters of pregnancy, *Magn. Reson. Med.* 80 (3) (2018) 1148–1157.
- [22] J.N. Stout, S. Rouhani, E.A. Turk, C.G. Ha, J. Luo, K. Rich, L.L. Wald, E. Adalsteinsson, W.H. Barth Jr., P.E. Grant, D.J. Roberts, Placental MRI: development of an MRI compatible ex vivo system for whole placenta dual perfusion, *Placenta* 101 (2020) 4–12.
- [23] A.A. Badachhpe, L. Devkota, I.V. Stupin, P. Sarkar, M. Srivastava, E.A. Tanifum, K.A. Fox, C. Yallampalli, A.V. Annapragada, K.B. Ghaghada, Nanoparticle contrast-enhanced T1-mapping enables estimation of placental fractional blood volume in a pregnant mouse model, *Sci. Rep.* 9 (1) (2019), 18707.
- [24] E.A. Turk, J. Luo, B. Gagoski, J. Pascau, C. Bibbo, J.N. Robinson, P.E. Grant, E. Adalsteinsson, P. Golland, N. Malpica, Spatiotemporal alignment of in utero BOLD-MRI series, *J. Magn. Reson. Imag.* 46 (2) (2017) 403–412.
- [25] A. Zhu, S.B. Reeder, K.M. Johnson, S.M. Nguyen, T.G. Golos, A. Shimakawa, M. R. Muehler, C.J. Francois, I.M. Bird, S.B. Fain, D.M. Shah, O. Wieben, D. Hernando, Evaluation of a motion-robust 2D chemical shift-encoded technique for R₂* and field map quantification in ferumoxytol-enhanced MRI of the

- placenta in pregnant rhesus macaques, *J. Magn. Reson. Imag.* 51 (2) (2020) 580–592.
- [26] X. Shao, D. Liu, T. Martin, T. Chanlaw, S.U. Devaskar, C. Janzen, A.M. Murphy, D. Margolis, K. Sung, D.J.J. Wang, Measuring human placental blood flow with multidelay 3D GRASE pseudocontinuous arterial spin labeling at 3T, *J. Magn. Reson. Imag.* 47 (6) (2018) 1667–1676.
- [27] A.A. Hartevelde, J. Hutter, S.L. Franklin, L.H. Jackson, M. Rutherford, J.V. Hajnal, M.J.P. van Osch, C. Bos, E. De Vita, Systematic evaluation of velocity-selective arterial spin labeling settings for placental perfusion measurement, *Magn. Reson. Med.* 84 (4) (2020) 1828–1843.
- [28] J.A. Salati, V.H.J. Roberts, M.C. Schabel, J.O. Lo, C.D. Kroenke, K. S. Lewandowski, J.R. Lindner, K.L. Grove, A.E. Frias, Maternal high-fat diet reversal improves placental hemodynamics in a nonhuman primate model of diet-induced obesity, *Int. J. Obes.* 43 (4) (2019) 906–916.
- [29] J.O. Lo, M.C. Schabel, V.H. Roberts, T.K. Morgan, J.P. Rasanen, C.D. Kroenke, S. R. Shoemaker, E.R. Spindel, A.E. Frias, Vitamin C supplementation ameliorates the adverse effects of nicotine on placental hemodynamics and histology in nonhuman primates, *Am. J. Obstet. Gynecol.* 212 (3) (2015), 370.e371–378.
- [30] C. Janzen, M.Y.Y. Lei, B.R. Lee, S. Vangala, I. DelRosario, Q. Meng, B. Ritz, J. Liu, M. Jerrett, T. Chanlaw, S. Choi, A. Aliabadi, P.A. Fortes, P.S. Sullivan, A. Murphy, G.D. Vecchio, S. Thamocharan, K. Sung, S.U. Devaskar, A description of the imaging innovations for placental assessment in response to environmental pollution study, *Am. J. Perinatol.* (2022), <https://doi.org/10.1055/a-1961-2059>.
- [31] K.D. Ludwig, S.B. Fain, S.M. Nguyen, T.G. Golos, S.B. Reeder, I.M. Bird, D. M. Shah, O.E. Wieben, K.M. Johnson, Perfusion of the placenta assessed using arterial spin labeling and ferumoxytol dynamic contrast enhanced magnetic resonance imaging in the rhesus macaque, *Magn. Reson. Med.* 81 (3) (2019) 1964–1978.
- [32] J.A. Macdonald, P.A. Corrado, S.M. Nguyen, K.M. Johnson, C.J. Francois, R. R. Magnus, D.M. Shah, T.G. Golos, O. Wieben, Uteroplacental and fetal 4D flow MRI in the pregnant rhesus macaque, *J. Magn. Reson. Imag.* 49 (2) (2019) 534–545.
- [33] D. Liu, X. Shao, A. Danyalov, T. Chanlaw, R. Masamed, D.J.J. Wang, C. Janzen, S. U. Devaskar, K. Sung, Human placenta blood flow during early gestation with pseudocontinuous arterial spin labeling MRI, *J. Magn. Reson. Imag.* 51 (4) (2020) 1247–1257.
- [34] Q. Bao, R. Hadas, S. Markovic, M. Neeman, L. Frydman, Diffusion and perfusion MRI of normal, preeclamptic and growth-restricted mice models reveal clear fetoplacental differences, *Sci. Rep.* 10 (1) (2020), 16380.
- [35] D.P. Seiter, S.M. Nguyen, T.K. Morgan, L. Mao, D.M. Dudley, D.H. O'Connor, M. E. Murphy, K.D. Ludwig, R. Chen, A. Dhyani, A. Zhu, M.L. Schotzko, K. G. Brunner, D.M. Shah, K.M. Johnson, T.G. Golos, O. Wieben, Ferumoxytol dynamic contrast enhanced magnetic resonance imaging identifies altered placental cotyledon perfusion in rhesus macaques†, *Biol. Reprod.* 107 (6) (2022) 1517–1527.
- [36] A. Palanisamy, T. Giri, J. Jiang, A. Bice, J.D. Quirk, S.B. Conyers, S.E. Maloney, N. Raghuraman, A.Q. Bauer, J.R. Garbow, D.F. Wozniak, In utero exposure to transient ischemia-hypoxemia promotes long-term neurodevelopmental abnormalities in male rat offspring, *JCI Insight* 5 (10) (2020).
- [37] J.O. Lo, M.C. Schabel, V.H. Roberts, X. Wang, K.S. Lewandowski, K.A. Grant, A. E. Frias, C.D. Kroenke, First trimester alcohol exposure alters placental perfusion and fetal oxygen availability affecting fetal growth and development in a non-human primate model, *Am. J. Obstet. Gynecol.* 216 (3) (2017), 302.e301–302.e308.
- [38] J.O. Lo, V.H.J. Roberts, M.C. Schabel, X. Wang, T.K. Morgan, Z. Liu, C. Studholme, C.D. Kroenke, A.E. Frias, Novel detection of placental insufficiency by magnetic resonance imaging in the nonhuman primate, *Reprod. Sci.* 25 (1) (2018) 64–73.
- [39] A.J. Hirsch, V.H.J. Roberts, P.L. Grigsby, N. Haese, M.C. Schabel, X. Wang, J. O. Lo, Z. Liu, C.D. Kroenke, J.L. Smith, M. Kelleher, R. Broecker, C.N. Kreklywich, C.J. Parkins, M. Denton, P. Smith, V. DeFilippis, W. Messer, J.A. Nelson, J. D. Hennebold, M. Grafe, L. Colgin, A. Lewis, R. Ducore, T. Swanson, A.W. Legasse, M.K. Axthelm, R. MacAllister, A.V. Moses, T.K. Morgan, A.E. Frias, D.N. Strelbow, Zika virus infection in pregnant rhesus macaques causes placental dysfunction and immunopathology, *Nat. Commun.* 9 (1) (2018) 263.
- [40] J.O. Lo, M.C. Schabel, V.H.J. Roberts, T.K. Morgan, S.S. Fei, L. Gao, K.G. Ray, K. S. Lewandowski, N.P. Newman, J.A. Bohn, K.A. Grant, A.E. Frias, C.D. Kroenke, Effects of early daily alcohol exposure on placental function and fetal growth in a rhesus macaque model, *Am. J. Obstet. Gynecol.* 226 (1) (2022), 130.e131–130.e111.
- [41] A. Ho, J. Hutter, P. Slatore, L. Jackson, P.T. Seed, L. McCabe, M. Al-Adnani, A. Marnerides, S. George, L. Story, J.V. Hajnal, M. Rutherford, L.C. Chappell, Placental magnetic resonance imaging in chronic hypertension: a case-control study, *Placenta* 104 (2021) 138–145.
- [42] J. Luo, E. Abaci Turk, C. Bibbo, B. Gagoski, D.J. Roberts, M. Vangel, C. M. Tempany-Afdhal, C. Barnewolt, J. Estroff, A. Palanisamy, W.H. Barth, C. Zera, N. Malpica, P. Golland, E. Adalsteinsson, J.N. Robinson, P.E. Grant, In vivo quantification of placental insufficiency by BOLD MRI: a human study, *Sci. Rep.* 7 (1) (2017) 3713.
- [43] T. Armstrong, D. Liu, T. Martin, R. Masamed, C. Janzen, C. Wong, T. Chanlaw, S. U. Devaskar, K. Sung, H.H. Wu, 3D R2* mapping of the placenta during early gestation using free-breathing multiecho stack-of-radial MRI at 3T, *J. Magn. Reson. Imag.* 49 (1) (2019) 291–303.
- [44] E. Abaci Turk, S.M. Abulnaga, J. Luo, J.N. Stout, H.A. Feldman, A. Turk, B. Gagoski, L.L. Wald, E. Adalsteinsson, D.J. Roberts, C. Bibbo, J.N. Robinson, P. Golland, P.E. Grant, W.H. Barth Jr., Placental MRI: effect of maternal position and uterine contractions on placental BOLD MRI measurements, *Placenta* 95 (2020) 69–77.
- [45] Z. Zun, K. Kapse, J. Quistorff, N. Andescavage, A.C. Gimovsky, H. Ahmadzia, C. Limperopoulos, Feasibility of QSM in the human placenta, *Magn. Reson. Med.* 85 (3) (2021) 1272–1281.
- [46] E. Abaci Turk, J.N. Stout, H.A. Feldman, B. Gagoski, C. Zhou, R. Tamen, M. K. Manhard, E. Adalsteinsson, D.J. Roberts, P. Golland, P.E. Grant, W.H. Barth Jr., Change in T2* measurements of placenta and fetal organs during Braxton Hicks contractions, *Placenta* 128 (2022) 69–71.
- [47] J. Hutter, P.J. Slatore, L. Jackson, A.D.S. Gomes, A. Ho, L. Story, J. O'Muircheartaigh, R. Teixeira, L.C. Chappell, D.C. Alexander, M.A. Rutherford, J.V. Hajnal, Multi-modal functional MRI to explore placental function over gestation, *Magn. Reson. Med.* 81 (2) (2019) 1191–1204.
- [48] A.E.P. Ho, J. Hutter, L.H. Jackson, P.T. Seed, L. McCabe, M. Al-Adnani, A. Marnerides, S. George, L. Story, J.V. Hajnal, M.A. Rutherford, L.C. Chappell, T2* placental magnetic resonance imaging in preterm preeclampsia: an observational cohort study, *Hypertension* 75 (6) (2020) 1523–1531.
- [49] J. Hutter, V. Kohli, N. Dellschaft, A. Uus, L. Story, J.K. Steinweg, P. Gowland, J. V. Hajnal, M.A. Rutherford, Dynamics of T2* and deformation in the placenta and myometrium during pre-labour contractions, *Sci. Rep.* 12 (1) (2022), 18542.
- [50] M.C. Schabel, V.H.J. Roberts, K.J. Gibbins, M. Rincon, J.E. Gaffney, A. D. Strelbow, A.M. Wright, J.O. Lo, B. Park, C.D. Kroenke, K. Szczotka, N.R. Blue, J.M. Page, K. Harvey, M.W. Varner, R.M. Silver, A.E. Frias, Quantitative longitudinal T2* mapping for assessing placental function and association with adverse pregnancy outcomes across gestation, *PLoS One* 17 (7) (2022), e0270360.
- [51] P.J. Slatore, J. Hutter, M. Palombo, L.H. Jackson, A. Ho, E. Panagiotaki, L. C. Chappell, M.A. Rutherford, J.V. Hajnal, D.C. Alexander, Combined diffusion-relaxometry MRI to identify dysfunction in the human placenta, *Magn. Reson. Med.* 82 (1) (2019) 95–106.
- [52] J.K. Steinweg, G.T.Y. Hui, M. Pietsch, A. Ho, M.P. van Poppel, D. Lloyd, K. Colford, J.M. Simpson, R. Razavi, K. Pushparajah, M. Rutherford, J. Hutter, T2* placental MRI in pregnancies complicated with fetal congenital heart disease, *Placenta* 108 (2021) 23–31.
- [53] J.N. Stout, C. Liao, B. Gagoski, E.A. Turk, H.A. Feldman, C. Bibbo, W.H. Barth Jr., S.A. Shinker, L.L. Wald, P.E. Grant, E. Adalsteinsson, Quantitative T1 (and T2) mapping by magnetic resonance fingerprinting (MRF) of the placenta before and after maternal hyperoxia, *Placenta* 114 (2021) 124–132.
- [54] J. Hutter, A. Ho, L.H. Jackson, P.J. Slatore, L.C. Chappell, J.V. Hajnal, M. A. Rutherford, An efficient and combined placental T1 -ADC acquisition in pregnancies with and without pre-eclampsia, *Magn. Reson. Med.* 86 (5) (2021) 2684–2691.
- [55] S. Markovic, A. Fages, T. Roussel, R. Hadas, A. Brandis, M. Neeman, L. Frydman, Placental physiology monitored by hyperpolarized dynamic (13)C magnetic resonance, *Proc. Natl. Acad. Sci. U. S. A.* 115 (10) (2018) E2429–e2436.
- [56] L.M. Smith, T.P. Wade, L.J. Friesen-Waldner, C.A. McKenzie, Optimizing SNR for multi-metabolite hyperpolarized carbon-13 MRI using a hybrid flip-angle scheme, *Magn. Reson. Med.* 84 (3) (2020) 1510–1517.
- [57] G. Farkash, S. Markovic, M. Novakovic, L. Frydman, Enhanced hyperpolarized chemical shift imaging based on a priori segmented information, *Magn. Reson. Med.* 81 (5) (2019) 3080–3093.
- [58] J. Luo, E. Abaci Turk, B. Gagoski, N. Copeland, I.Y. Zhou, V. Young, C. Bibbo, J. N. Robinson, C. Zera, W.H. Barth Jr., D.J. Roberts, P.Z. Sun, P.E. Grant, Preliminary evaluation of dynamic glucose enhanced MRI of the human placenta during glucose tolerance test, *Quant. Imag. Med. Surg.* 9 (10) (2019) 1619–1627.
- [59] A.A. Badachhape, A. Kumar, K.B. Ghaghada, I.V. Stupin, M. Srivastava, L. Devkota, Z. Starosolski, E.A. Tanifum, V. George, K.A. Fox, C. Yallampalli, A. V. Annapragada, Pre-clinical magnetic resonance imaging of retroplacental clear space throughout gestation, *Placenta* 77 (2019) 1–7.
- [60] S.M. Abulnaga, E.A. Turk, M. Bessmeltsev, P.E. Grant, J. Solomon, P. Golland, Volumetric parameterization of the placenta to a flattened template, *IEEE Trans. Med. Imag.* 41 (4) (2022) 925–936.
- [61] A.A. Badachhape, P. Bhandari, L. Devkota, M. Srivastava, E.A. Tanifum, V. George, K.A. Fox, C. Yallampalli, A.V. Annapragada, K.B. Ghaghada, Nanoparticle contrast-enhanced MRI for visualization of retroplacental clear space disruption in a mouse model of placental accreta spectrum (PAS), *Acad. Radiol.* (2022).
- [62] Y. Liu, F. Zabihollahy, R. Yan, B. Lee, C. Janzen, S.U. Devaskar, K. Sung, Evaluation of spatial attentive deep learning for automatic placental segmentation on longitudinal MRI, *J. Magn. Reson. Imag.* 57 (5) (2023) 1533–1540.
- [63] K.B. Ghaghada, Z.A. Starosolski, S. Bhayana, I. Stupin, C.V. Patel, R.C. Bhavane, H. Gao, A. Bednov, C. Yallampalli, M. Belfort, V. George, A.V. Annapragada, Pre-clinical evaluation of a nanoparticle-based blood-pool contrast agent for MR imaging of the placenta, *Placenta* 57 (2017) 60–70.
- [64] A. Ho, L.C. Chappell, L. Story, M. Al-Adnani, A. Eglhoff, E. Routledge, M. Rutherford, J. Hutter, Visual assessment of the placenta in antenatal magnetic resonance imaging across gestation in normal and compromised pregnancies: observations from a large cohort study, *Placenta* 117 (2022) 29–38.
- [65] A. Rahman, Y.Q. Zhou, Y. Yee, J. Dazai, L.S. Cahill, J. Kingdom, C.K. Macgowan, J.G. Sled, Ultrasound detection of altered placental vascular morphology based on hemodynamic pulse wave reflection, *Am. J. Physiol. Heart Circ. Physiol.* 312 (5) (2017) H1021–h1029.
- [66] K. Kuo, V.H.J. Roberts, J. Gaffney, D.L. Takahashi, T. Morgan, J.O. Lo, R. L. Stouffer, A.E. Frias, Maternal high-fat diet consumption and chronic

- hyperandrogenemia are associated with placental dysfunction in female rhesus macaques, *Endocrinology* 160 (8) (2019) 1937–1949.
- [67] L.S. Cahill, Y.Q. Zhou, J. Hoggarth, L.X. Yu, A. Rahman, G. Stortz, C. L. Whitehead, A. Baschat, J.C. Kingdom, C.K. Macgowan, L. Serghides, J.G. Sled, Placental vascular abnormalities in the mouse alter umbilical artery wave reflections, *Am. J. Physiol. Heart Circ. Physiol.* 316 (3) (2019) H664–h672.
- [68] L.S. Cahill, C.L. Whitehead, S.R. Hobson, G. Stortz, J.C. Kingdom, A. Baschat, K. E. Murphy, L. Serghides, C.K. Macgowan, J.G. Sled, Effect of maternal betamethasone administration on feto-placental vascular resistance in the mouse, *Biol. Reprod.* 101 (4) (2019) 823–831.
- [69] J.G. Sled, G. Stortz, L.S. Cahill, N. Milligan, V. Ayyathurai, L. Serghides, E. Morgen, V. Seravalli, C. Delp, C. McShane, A. Baschat, J. Kingdom, C. K. Macgowan, Reflected hemodynamic waves influence the pattern of Doppler ultrasound waveforms along the umbilical arteries, *Am. J. Physiol. Heart Circ. Physiol.* 316 (5) (2019) H1105–h1112.
- [70] G. Stortz, L.S. Cahill, A.R. Chandran, A. Baschat, J.G. Sled, C.K. Macgowan, Quantification of wave reflection in the human umbilical artery from asynchronous Doppler ultrasound measurements, *IEEE Trans. Med. Imag.* 39 (11) (2020) 3749–3757.
- [71] L. Paranavitana, M. Walker, A.R. Chandran, N. Milligan, S. Shinar, C. L. Whitehead, S.R. Hobson, L. Serghides, W.T. Parks, A.A. Baschat, C. K. Macgowan, J.G. Sled, J.C. Kingdom, L.S. Cahill, Sex differences in uterine artery Doppler during gestation in pregnancies complicated by placental dysfunction, *Biol. Sex Differ.* 12 (1) (2021) 19.
- [72] L.S. Cahill, G. Stortz, A. Ravi Chandran, N. Milligan, S. Shinar, C.L. Whitehead, S. R. Hobson, V. Ayyathurai, A. Rahman, R. Saghian, K.J. Jobst, C. McShane, D. Block-Abraham, V. Seravalli, M. Laurie, S. Millard, C. Delp, D. Wolfson, A. A. Baschat, K.E. Murphy, L. Serghides, E. Morgen, C.K. Macgowan, W.T. Parks, J. C. Kingdom, J.G. Sled, Wave reflections in the umbilical artery measured by Doppler ultrasound as a novel predictor of placental pathology, *EBioMedicine* 67 (2021), 103326.
- [73] A.O. Odibo, U. Kayisli, Y. Lu, O. Kayisli, F. Schatz, L. Odibo, H. Chen, R. Bronsteen, C.J. Lockwood, Longitudinal assessment of spiral artery and intravillous arteriole blood flow and adverse pregnancy outcome, *Ultrasound Obstet. Gynecol.* 59 (3) (2022) 350–357.
- [74] R. Saghian, L. Cahill, A. Rahman, J. Steinman, G. Stortz, J. Kingdom, C. Macgowan, J. Sled, Interpretation of wave reflections in the umbilical arterial segment of the feto-placental circulation: computational modeling of the feto-placental arterial tree, *IEEE Trans. Biomed. Eng.* 68 (12) (2021) 3647–3658.
- [75] R. Saghian, J.L. James, M.H. Tawhai, S.L. Collins, A.R. Clark, Association of placental jets and mega-jets with reduced villous density, *J. Biomech. Eng.* 139 (5) (2017) 510011–5100110.
- [76] S.L. Collins, G.N. Stevenson, A. Al-Khan, N.P. Illsley, L. Impey, L. Pappas, S. Zamudio, Three-dimensional power Doppler ultrasonography for diagnosing abnormally invasive placenta and quantifying the risk, *Obstet. Gynecol.* 126 (3) (2015) 645–653.
- [77] H. Maynard, S. Zamudio, E. Jauniaux, S.L. Collins, The importance of bladder volume in the ultrasound diagnosis of placenta accreta spectrum disorders, *Int. J. Gynaecol. Obstet.* 140 (3) (2018) 332–337.
- [78] N. Schwartz, J. Siegal, A. Rourke, C.M. Sehgal, Placental pulsatility: quantitative assessment of placental bed vasculature by 2-dimensional Doppler cine imaging, *J. Ultrasound Med.* 38 (2) (2019) 471–479.
- [79] G.N. Stevenson, J.A. Noble, A.W. Welsh, L. Impey, S.L. Collins, Automated visualization and quantification of spiral artery blood flow entering the first-trimester placenta, using 3-D power Doppler ultrasound, *Ultrasound Med. Biol.* 44 (3) (2018) 522–531.
- [80] S.L. Collins, A.W. Welsh, L. Impey, J.A. Noble, G.N. Stevenson, 3D fractional moving blood volume (3D-FMBV) demonstrates decreased first trimester placental vascularity in pre-eclampsia but not the term, small for gestation age baby, *PLoS One* 12 (6) (2017), e0178675.
- [81] Y. Yin, P. Looney, S.L. Collins, Standardization of blood flow measurements by automated vascular analysis from power Doppler ultrasound scan, *Proc. SPIE-Int. Soc. Opt. Eng.* (2020), 11314.
- [82] L. Wang, J.M. Cochran, T. Ko, W.B. Baker, K. Abramson, L. He, D.R. Busch, V. Kavuri, R.L. Linn, S. Parry, A.G. Yodh, N. Schwartz, Non-invasive monitoring of blood oxygenation in human placentas via concurrent diffuse optical spectroscopy and ultrasound imaging, *Nat. Biomed. Eng.* 6 (9) (2022) 1017–1030.
- [83] H. Qi, S. Collins, A. Noble, Weakly supervised learning of placental ultrasound images with residual networks, in: *Med Image Underst Anal Conf* (2017), vol. 723, 2017, pp. 98–108.
- [84] H. Qi, S. Collins, J.A. Noble, Automatic lacunae localization in placental ultrasound images via layer aggregation, *Med Image Comput Assist Interv* 11071 (2018) 921–929.
- [85] H. Qi, S. Collins, J.A. Noble, Knowledge-guided pretext learning for utero-placental interface detection, *Med Image Comput Assist Interv* 12261 (2020) 582–593.
- [86] P. Looney, G.N. Stevenson, K.H. Nicolaidis, W. Plasencia, M. Molloholli, S. Natsis, S.L. Collins, Fully automated, real-time 3D ultrasound segmentation to estimate first trimester placental volume using deep learning, *JCI Insight* 3 (11) (2018).
- [87] P. Looney, Y. Yin, S.L. Collins, K.H. Nicolaidis, W. Plasencia, M. Molloholli, S. Natsis, G.N. Stevenson, Fully automated 3-D ultrasound segmentation of the placenta, amniotic fluid, and fetus for early pregnancy assessment, *IEEE Trans. Ultrason. Ferroelectrics Freq. Control* 68 (6) (2021) 2038–2047.
- [88] I. Oguz, N. Yushkevich, A. Pouch, B.U. Oguz, J. Wang, S. Parameshwaran, J. Gee, P.A. Yushkevich, N. Schwartz, Minimally interactive placenta segmentation from three-dimensional ultrasound images, *J. Med. Imaging* 7 (1) (2020), 014004.
- [89] N. Schwartz, I. Oguz, J. Wang, A. Pouch, N. Yushkevich, S. Parameshwaran, J. Gee, P. Yushkevich, B. Oguz, Fully automated placental volume quantification from 3D ultrasound for prediction of small-for-gestational-age infants, *J. Ultrasound Med.* 41 (6) (2022) 1509–1524.
- [90] M.Y. Rennie, L.S. Cahill, S.L. Adamson, J.G. Sled, Arterio-venous fetoplacental vascular geometry and hemodynamics in the mouse placenta, *Placenta* 58 (2017) 46–51.
- [91] L.S. Cahill, M.Y. Rennie, J. Hoggarth, L.X. Yu, A. Rahman, J.C. Kingdom, M. Seed, C.K. Macgowan, J.G. Sled, Feto- and utero-placental vascular adaptations to chronic maternal hypoxia in the mouse, *J. Physiol.* 596 (15) (2018) 3285–3297.
- [92] R. Saghian, L.S. Cahill, S.K. Debebe, A. Rahman, L. Serghides, C.R. McDonald, A. M. Weckman, K.C. Kain, J.G. Sled, Allometric scaling relationships in mouse placenta, *J. R. Soc. Interface* 19 (196) (2022), 20220579.
- [93] A. Al-Khan, G. Guirguis, S. Zamudio, M. Alvarez, K. Martimucci, D. Luke, J. Alvarez-Perez, Preoperative cystoscopy could determine the severity of placenta accreta spectrum disorders: an observational study, *J. Obstet. Gynaecol. Res.* 45 (1) (2019) 126–132.
- [94] L.M. Yamaleyeva, Y. Sun, T. Bledsoe, A. Hoke, S.B. Gurley, K.B. Brosnihan, Photoacoustic imaging for in vivo quantification of placental oxygenation in mice, *Faseb. J.* 31 (12) (2017) 5520–5529.
- [95] V.H. Roberts, A.E. Frias, Contrast-enhanced ultrasound for the assessment of placental development and function, *Biotechniques* 69 (5) (2020) 392–399.
- [96] S. Mathewlynn, S.L. Collins, Volume and vascularity: using ultrasound to unlock the secrets of the first trimester placenta, *Placenta* 84 (2019) 32–36.
- [97] P.H.B. Diniz, Y. Yin, S. Collins, Deep learning strategies for ultrasound in pregnancy, *Eur Med J Reprod Health* 6 (1) (2020) 73–80.
- [98] E. Abaci Turk, J.N. Stout, C. Ha, J. Luo, B. Gagoski, F. Yetisir, P. Golland, L. L. Wald, E. Adalsteinsson, J.N. Robinson, D.J. Roberts, W.H. Barth Jr., P.E. Grant, Placental MRI: developing accurate quantitative measures of oxygenation, *Top. Magn. Reson. Imag.* 28 (5) (2019) 285–297.
- [99] A.V. Dimov, J. Li, T.D. Nguyen, A.G. Roberts, P. Spincemaille, S. Straub, Z. Zun, M.R. Prince, Y. Wang, QSM throughout the body, *J. Magn. Reson. Imag.* 57 (6) (2023) 1621–1640.
- [100] L.M. Yamaleyeva, K.B. Brosnihan, L.M. Smith, Y. Sun, Preclinical ultrasound-guided photoacoustic imaging of the placenta in normal and pathologic pregnancy, *Mol. Imag.* 17 (2018), 1536012118802721.
- [101] P. Slator, R. Aughwane, G. Cade, D. Taylor, A.L. David, R. Lewis, E. Jauniaux, A. Desjardins, L.J. Salomon, A.E. Millischer, V. Tsatsaris, M. Rutherford, E. D. Johnstone, A. Melbourne, Placenta imaging workshop 2018 report: multiscale and multimodal approaches, *Placenta* 79 (2019) 78–82.
- [102] E. Abaci Turk, S.M. Abulnaga, J. Luo, J.N. Stout, H.A. Feldman, A. Turk, B. Gagoski, L.L. Wald, E. Adalsteinsson, D.J. Roberts, C. Bibbo, J.N. Robinson, P. Golland, P.E. Grant, W.H. Barth Jr., Corrigendum to "Placental MRI: effect of maternal position and uterine contractions on placental BOLD MRI measurements" [*Placenta* 95 (2020) 69–77], *Placenta* 100 (2020) 171–172.
- [103] A. Ho, L.C. Chappell, L. Story, M. Al-Adnani, A. Egloff, E. Routledge, M. Rutherford, J. Hutter, Corrigendum to "Visual assessment of the placenta in antenatal magnetic resonance imaging across gestation in normal and compromised pregnancies: observations from a large cohort study" [17 January 2022 29–38], *Placenta* 119 (2022) 31.
- [104] J. Jackson, V. George, J. McKinney, K.A. Fox, Multimodal postpartum imaging of a severe case of Couvelaire uterus, *Case Rep. Perinat. Med.* 11 (1) (2022), 20210013.
- [105] P.M. Bossuyt, J.B. Reitsma, D.E. Bruns, C.A. Gatsonis, P.P. Glasziou, L. Irwig, J. G. Lijmer, D. Moher, D. Rennie, H.C. de Vet, H.Y. Kressel, N. Rifai, R.M. Golub, D. G. Altman, L. Hooft, D.A. Korevaar, J.F. Cohen, STARD 2015: an updated list of essential items for reporting diagnostic accuracy studies, *BMJ* 351 (2015) h5527.
- [106] K. Smith, Women's health research lacks funding - in a series of charts, *Nature* 617 (7959) (2023) 28–29.